AIP Advances

Universal formalism of Fano resonance

Liang Huang, Ying-Cheng Lai, Hong-Gang Luo, and Celso Grebogi

Citation: AIP Advances **5**, 017137 (2015); doi: 10.1063/1.4906797
View online: http://dx.doi.org/10.1063/1.4906797
View Table of Contents: http://scitation.aip.org/content/aip/journal/adva/5/1?ver=pdfcov
Published by the AIP Publishing

Universal formalism of Fano resonance

Liang Huang,[1] Ying-Cheng Lai,[2,3,4] Hong-Gang Luo,[1,5] and Celso Grebogi[4]
[1]*School of Physical Science and Technology and Key Laboratory for Magnetism and Magnetic Materials of MOE, Lanzhou University, Lanzhou, Gansu 730000, China*
[2]*School of Electrical, Computer, and Energy Engineering, Arizona State University, Tempe, Arizona 85287, USA*
[3]*Department of Physics, Arizona State University, Tempe, Arizona 85287, USA*
[4]*Institute for Complex Systems and Mathematical Biology, King's College, University of Aberdeen, Aberdeen AB24 3UE, UK*
[5]*Beijing Computational Science Research Center, Beijing 100084, China*

(Received 23 November 2014; accepted 15 January 2015; published online 28 January 2015)

The phenomenon of Fano resonance is ubiquitous in a large variety of wave scattering systems, where the resonance profile is typically asymmetric. Whether the parameter characterizing the asymmetry should be complex or real is an issue of great experimental interest. Using coherent quantum transport as a paradigm and taking into account of the collective contribution from all available scattering channels, we derive a universal formula for the Fano-resonance profile. We show that our formula bridges naturally the traditional Fano formulas with complex and real asymmetry parameters, indicating that the two types of formulas are fundamentally equivalent (except for an offset). The connection also reveals a clear footprint for the conductance resonance during a dephasing process. Therefore, the emergence of complex asymmetric parameter when fitting with experimental data needs to be properly interpreted. Furthermore, we have provided a theory for the width of the resonance, which relates explicitly the width to the degree of localization of the close-by eigenstates and the corresponding coupling matrices or the self-energies caused by the leads. Our work not only resolves the issue about the nature of the asymmetry parameter, but also provides deeper physical insights into the origin of Fano resonance. Since the only assumption in our treatment is that the transport can be described by the Green's function formalism, our results are also valid for broad disciplines including scattering problems of electromagnetic waves, acoustics, and seismology. [http://dx.doi.org/10.1063/1.4906797]

I. INTRODUCTION

A fundamental phenomenon associated with quantum or wave scattering dynamics is Fano resonance.[1,2] A typical scattering system consists of incoming channels, a scatterer or a conductor, and outgoing channels. The scatterer, when isolated, can be regarded as a closed system with a discrete spectrum of intrinsic energy levels. When the energy of the incoming particle or wave matches an energy level, a resonant behavior can arise in some experimentally measurable quantities, such as the conductance in a quantum-transport system. The resonance profile is typically asymmetric, and can in general be expressed as $(\varepsilon + q)^2/(\varepsilon^2 + 1)$, where ε is the normalized energy deviation from the center of the resonance, and q is the parameter characterizing the degree of asymmetry of the resonance. The asymmetry parameter q is of great experimental importance as it determines how the experimental data can be fitted by the Fano profile.

The profile was first derived by Fano[1] in the study of inelastic scattering of electrons off the helium atom and auto-ionization, although the phenomenon was predicted earlier in elastic neutron scattering.[3] Being a general wave interference phenomenon, Fano resonance has been found in many contexts in physics, such as photon-ionization,[4] Raman scattering,[5,6] photon-absorption in quantum-well structure,[7,8] scanning microscopy tunneling in the presence of impurity,[9–11] transport through

a single-electron transistor[12] and through the Aharnov-Bohm interferometer,[13–16] transport through crossed carbon nanotubes,[17,18] microwave scattering,[19] plasmonic nanostructures and metamaterials,[20] and optical resonances.[21–24] Applications exploiting Fano resonance have even been proposed for biochemical sensors.[25]

Although it is of high experimental relevance, the issue that whether the asymmetric parameter q should be real or complex remains confusing in the literature.[26] For example, it was demonstrated that, in single-channel scattering quantum-transport systems, q is strictly real if the time-reversal symmetry (TRS) is preserved.[27] When the TRS is broken, q will generally be complex,[27] which was observed experimentally in an Aharnov-Bohm interferometer with a quantum dot embedded in one of the arms.[15,16] With a changing magnetic field, q oscillates, which was explained[28] but again by using the single-channel scattering model. Later, it was shown that for multi-channel scattering, q is in general complex even when TRS is NOT broken.[29] It was also proposed[27] that the complex q parameter can be used to characterize the dephasing time. The variation in q and the degree of decoherence were studied in microwave billiards where a non-zero imaginary part of q was declared.[19] Moreover, it was suggested that the trajectory of q in its complex plane could be used to probe whether the decoherence is caused by dissipation or dephasing.[30] Complex q parameter was used in other contexts as well, such as the second-order effects in helium auto-ionization excited by electron impact[31] and ultrashort laser excitation in the bismuth single crystal.[32]

The above theoretical investigations of the Fano line shape in the conductance all employed the calculation of the transmission coefficient of a particular scattering channel, namely, $|t_{nm}|^2$. Since for different channels the resonant line profile can be quite different,[28,29] the final line shape summing over all possible channels is still undetermined.

In this paper, we derive the asymmetric Fano resonance profile using the Green's function method to calculate the transmission, taking into account of all transmission channels, and address the question of whether the fundamental q parameter should be complex or real. To be concrete, we focus on low-dimensional quantum-transport systems exemplified by quantum dots or quantum point contacts. Despite the relatively long history of research on Fano resonance, for quantum transport systems the asymmetric profile has been studied much later.[12,33–35] Our approach to probing into the nature of the q parameter consists of two steps. First, by using the non-equilibrium Green's function to calculate, for all scattering channels, the transmission as a function of the Fermi energy, we derive a formula for the resonance profile and verify it numerically using graphene quantum dot systems. The key approximation employed is that the self-energy terms and the coupling functions are slow variables, so for energy near an isolated resonance, the Green's function can be decomposed into a fast and a slowly varying components. Second, we show that our formula bridges naturally the conventional Fano formulas with complex and real q parameters. In particular, we find a simple mathematical transform that can convert the Fano formula with complex q parameter to our formula, and another transform that turns our formula into the Fano formula with real q parameter. The implication is that, for any experimental situation the conventional Fano formulas with complex or real q parameter are equally applicable, given that an offset can be added to the real q Fano formula, which is common in fitting experimental data.[12,15,16,36,37] Our investigation also leads to an expression of the width of the resonance, which is explicitly related to the degree of localization of the close-by eigenstates for the closed system and the corresponding coupling matrices or the self-energies caused by the leads. Since the self-energies are slow variables, the width depends mostly on the eigenstates, i.e., if the eigenstates is highly localized, then its values at the boundary will be minimum and the cross integration with the self-energies will be significantly small, leading to sharp resonances.

In our analysis, no detailed information about the specific system is required. Thus, our formula and its direct consequence hold for any coherent transport dynamics for both bosons and fermions. Especially, for bosons, i.e., phonons, the control parameter is not the energy but the frequency, thus requiring only a straightforward modification in our formula. For fermion transport, our formula is valid for small-scale electronic devices such as quantum-dot systems, quantum point contacts, nano-scale heterostructures, and single-molecule transport devices.

The rest of the paper is organized as follows. Section II derives the profile of the Fano resonance starting from the general frame work of calculating transmission and discusses the connection to the well-known Fano formula with both real and complex asymmetric parameters. Section III provides an

approximate expression of the width of the Fano resonance with a clear physical picture, which relates the strong localized scar/pointer[38–42] states to sharp conductance fluctuations. Concluding remarks are then presented in Sec. IV.

II. THE FANO RESONANCE

A. General scheme for quantum transport

Without loss of generality, we consider a two-terminal quantum-dot system, which can be formulated as follows.[43] The system is divided into three parts: left lead, conductor (scatterer) of arbitrary shape, and right lead, where the semi-infinite left and right multi-mode electronic waveguides are assumed to be uniform, connected only to the conductor (or the scattering region), as shown in Fig. 1. The conductor is chosen to include all the irregular components in the scattering system such as geometrical shape, arbitrary electric or magnetic potential, and/or disorder, etc. The conductor can be a single molecule, a quantum dot, or any other small-scale structure through which electronic waves pass coherently. The tight-binding Hamiltonian matrix can then be written as

$$H = \begin{pmatrix} H_L & H_{LC} & 0 \\ H_{CL} & H_C & H_{CR} \\ 0 & H_{RC} & H_R \end{pmatrix}, \tag{1}$$

where H_C is a finite-size square matrix of dimension $N_C \times N_C$, N_C is the number of discrete points in the conductor, and $H_{L,R}$ are the Hamiltonians of the left and right leads, respectively. The various couplings between the conductor and leads are given by the matrices H_{LC}, H_{CL}, H_{CR}, and H_{RC}.

The effect of the semi-infinite uniform leads can be treated by using non-Hermitian self-energy terms, Σ_L, Σ_R, for the left and right leads, respectively, which are determined by

$$\Sigma_L \equiv H_{CL} G_L H_{LC}, \quad \text{and} \quad \Sigma_R \equiv H_{CR} G_R H_{RC}, \tag{2}$$

where $G_{L,R}$ are Green's functions for the left and the right leads. For practical analysis, the self-energies can be calculated efficiently using some standard recursive method.[44–46]

The retarded Green's function for the conductor is given by

$$G_C(E) = (EI - H_C - \Sigma)^{-1}, \tag{3}$$

where $\Sigma = \Sigma_L + \Sigma_R$ is the total self-energy from both leads. The coupling matrices $\Gamma_L(E)$ and $\Gamma_R(E)$ are the difference between the retarded and the advanced self-energy:

$$\Gamma_{L,R} = i(\Sigma_{L,R} - \Sigma_{L,R}^{\dagger}), \tag{4}$$

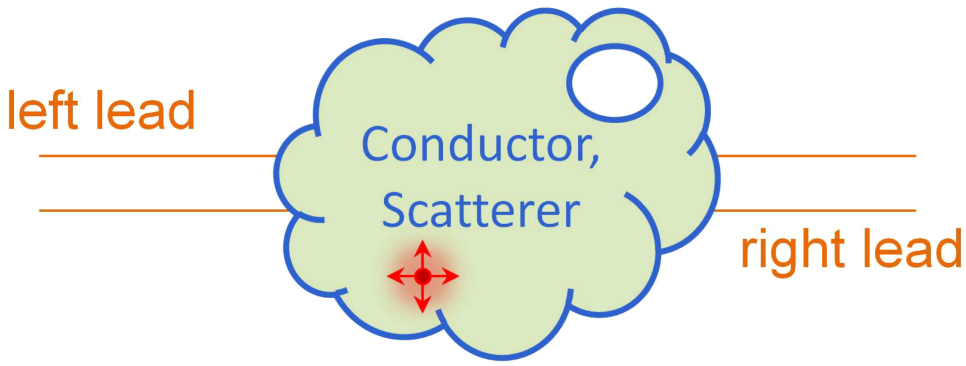

FIG. 1. A general scheme for transport through a conductor or a scatterer connected with two semi-infinite leads. The leads are assumed to be uniform. The conductor contains any irregular component of the scattering system. For example, it can be a scatterer with a nonuniform shape, or with a whole that mimics the Aharonv-Bohm interferometer, or with irregular electric or magnetic potential or disorders, or a single molecule.

which characterize the coupling between the conductor and the leads, and are Hermitian: $\Gamma_{L,R}^{\dagger} = \Gamma_{L,R}$. For notational convenience, we write $G_C \equiv G$.

The quantum transmission $T(E)$, as a function of the Fermi energy, is given by[43]

$$T(E) = \mathrm{Tr}[\Gamma_L(E)G(E)\Gamma_R(E)(G(E))^{\dagger}]. \tag{5}$$

The classic Landauer's formula[47] can then be used to calculate the conductance:

$$G(E_F) = \frac{2e^2}{h}\int T(E)\Big(-\frac{\partial f}{\partial E}\Big)dE, \tag{6}$$

where $T(E)$ is the transmission of the conductor and $f(E) = 1/[1 + e^{(E-E_F)/kT}]$ is the Fermi distribution function. At low temperature, $-\partial f/\partial E \approx \delta(E - E_F)$, thus $G(E_F) = (2e^2/h)T(E_F)$. To be concrete, we focus on the low-temperature conductance, or equivalently, the transmission T.

B. Fast-slow expansion

To analyze the Fano resonance profile, the scales of variations (e.g., fast or slow with respect to the energy variation) of the various quantities in Eq. (5) are the key. Indeed, the self-energy Σ varies slowly with the energy, so do the coupling matrices $\Gamma_{L,R}$. That is, in the energy scale where the transmission exhibits rapid, nearly abrupt oscillations, e.g., through a Fano resonance, the value of the self-energy matrix elements can be regarded as approximately constant, as shown in Fig. 2. The change in the transmission must then come from the energy-dependence of the Green's function $G(E)$. Our idea to probe into the Fano resonance profile is then to consider a small energy range about such a resonance and decompose the Green's function $G(E)$ into two components: $G(E) = G_0(E) + G_1(E)$, where $G_0(E)$ and $G_1(E)$ are the slow and fast components, respectively. The transmission can then

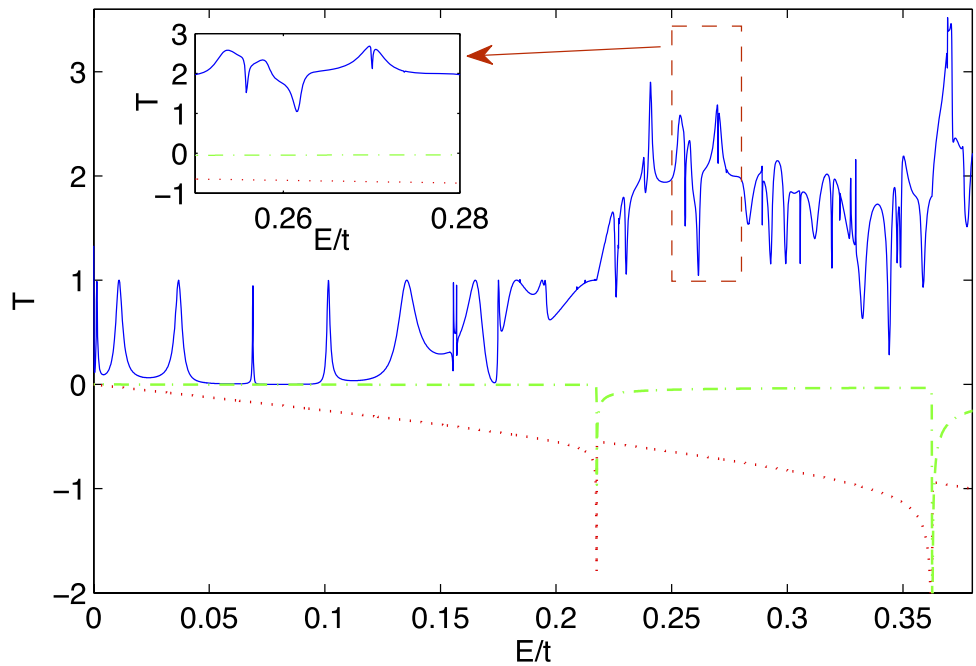

FIG. 2. For a graphene quantum dot, a demonstration of the slow variation of the self-energy through a Fano resonance, where the solid curve is transmission versus E with sharp resonances, the dotted and dash-dotted curves denote the real and imaginary parts of an arbitrary element of the self-energy matrix, respectively. The spikes in the self-energy indicate the energy value at which the number of the transmitting modes in the leads increases. The inset shows a zoom-in with a few transmission resonances. It can be seen that in any small energy interval about a single resonance, the self-energy can be regarded as a constant.

be expressed as

$$\begin{aligned} T &= \mathrm{Tr}[\Gamma_L G_0 \Gamma_R (G_0)^\dagger] + \mathrm{Tr}[\Gamma_L G_0 \Gamma_R (G_1)^\dagger] \\ &\quad + \mathrm{Tr}[\Gamma_L G_1 \Gamma_R (G_0)^\dagger] + \mathrm{Tr}[\Gamma_L G_1 \Gamma_R (G_1)^\dagger] \\ &= T_{00} + T_{01} + T_{10} + T_{11}, \end{aligned} \tag{7}$$

where Γ_L, Γ_R, and $G_0(E)$ are treated as constant matrices. Among the four terms in Eq. (7), only T_{00} varies slowly with the energy. Unlike the standard perturbation theory, here $G_1(E)$ is the fast changing component of the Green's function, but it is not necessarily small. Thus the remaining three terms T_{01}, T_{10}, and T_{11} exhibit approximately the same behaviors in terms of their magnitudes and rates of change with the energy. Consequently, T_{11} cannot be regarded as a second-order term. Note that T_{01} and T_{10} are not independent of each other:

$$\begin{aligned} T_{01}^\dagger &= \left(\mathrm{Tr}[\Gamma_L G_0 \Gamma_R (G_1)^\dagger]\right)^\dagger \\ &= \mathrm{Tr}[(G_1)(\Gamma_R)^\dagger (G_0)^\dagger (\Gamma_L)^\dagger] \\ &= \mathrm{Tr}[\Gamma_L G_1 \Gamma_R (G_0)^\dagger] = T_{10}, \end{aligned}$$

where we have used the relation $\Gamma_{L,R}^\dagger = \Gamma_{L,R}$ and the invariant property of trace under cyclic permutations. Similarly, we have $T_{11}^\dagger = T_{11}$ so that T_{11} is real.

C. Construction of G_1

The Green's function can be expressed in matrix form as[43] $G(E) = \sum_\alpha \Psi_\alpha \Phi_\alpha^\dagger / (E - \varepsilon_\alpha)$, where the summation is over all the eigenstates, Ψ_α and Φ_α are the right and left eigenvectors associated with the eigenvalue ε_α of the generalized Hamiltonian matrix $(H_C + \Sigma)$: $[H_C + \Sigma]\Psi_\alpha = \varepsilon_\alpha \Psi_\alpha, \Phi_\alpha^\dagger [H_C + \Sigma] = \varepsilon_\alpha \Phi_\alpha^\dagger$. In general, the self-energy is not Hermitian and, hence, Ψ_α and Φ_α are not identical but form a bi-orthogonal set: $\Phi_\alpha^\dagger \Psi_\beta = \delta_{\alpha,\beta}$. The eigenvalues ε_α are generally complex: $\varepsilon_\alpha = E_\alpha - i\gamma_\alpha$, where the imaginary part originates from the self-energy and characterizes the lifetime of the corresponding state before it tunnels into the leads.

Consider a small energy interval that contains a transmission resonance, in which $G(E)$ can be decomposed into a slowly varying and a fast changing components: $G(E) = G_0(E) + G_1(E)$. Let E_0 denote the center of the resonance. In the small energy interval about E_0, we can identify a small set Ω_0 of eigenstates and write $G_1(E) = \sum_{\alpha \in \Omega_0} \Psi_\alpha \Phi_\alpha^\dagger / (E - \varepsilon_\alpha)$, and the summation over all the other eigenstates can be denoted as $G_0(E)$. $G_1(E)$ is the fast component because, for E around E_0, only those states whose energies are close to E_0 will contribute to the variation of $G(E)$. Note that although the identification of Ω_0 can be somewhat arbitrary, practically, when an eigenstate is well separated from others and the corresponding eigenvalue has a small imaginary part, i.e., $\gamma_\alpha < E_{\alpha+1} - E_\alpha$ and $\gamma_\alpha < E_\alpha - E_{\alpha-1}$, it will result in a transmission resonance by itself with energy scale γ_α, as shown in Fig. 3. In this case, Ω_0 can be chosen to have only one eigenstate α. This will be our focus in the following derivation of the resonance profile.

Situation can also arise where the eigenenergies of a small number of eigenstates are close to each other and have large γ_α values, i.e., γ_α is larger than the spacing between the real parts of adjacent eigenvalues. In this case, the transmission resonances from these eigenstates are not separable, and the resulting resonance profile is the mixture of the isolated profiles.

D. The universal formula

For a single separated resonance, $G_1(E)$ is given by:

$$G_1(E) = \frac{\Psi_\alpha \Phi_\alpha^\dagger}{E - \varepsilon_\alpha}, \tag{8}$$

and $G_0(E)$ can be regarded as a constant matrix and approximated by its value at E_0: $G_0(E) \approx G_0(E_0) = G(E_0) - G_1(E_0) \equiv G_0$, where $G(E_0) = [E_0 I - H_C - \Sigma(E_0)]^{-1}$. Alternatively, the Green's function

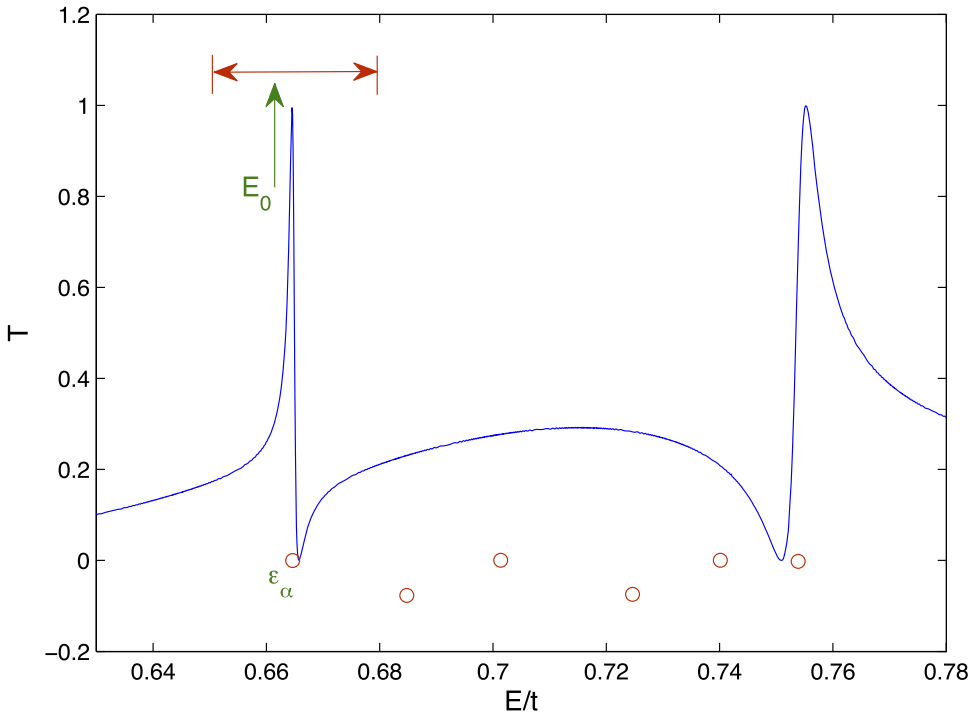

FIG. 3. Identification of the eigenstate set Ω_0: for the same graphene quantum dot in Fig. 1 in the main text, transmission versus energy in a small interval that contains two Fano resonances. The circles below the curve indicate the locations of $\varepsilon_\alpha = E_\alpha - i\gamma_\alpha$. There is a well separated resonance profile about E_0, which occurs at ε_α.

can be expressed as

$$G(E) \approx G_0 + G_1(E) = G_0 + \frac{\Psi_\alpha \Phi_\alpha^\dagger}{E - \varepsilon_\alpha}.$$

The coupling matrices vary slowly with the energy and can be regarded as constant matrices evaluated at E_0 as well:

$$\Gamma_{L,R}(E) \approx \Gamma_{L,R}(E_0) = i[\Sigma_{L,R}(E_0) - \Sigma_{L,R}^\dagger(E_0)].$$

With the separation of the various quantities into slow and fast components, we can express the transmission $T(E)$ as

$$\begin{aligned}
T\ (E) &= \mathrm{Tr}[\Gamma_L(E)G(E)\Gamma_R(E)(G(E))^\dagger] \\
&\approx \mathrm{Tr}[\Gamma_L(E_0)(G_0 + G_1(E))\Gamma_R(E_0)(G_0 + G_1(E))^\dagger] \\
&= \mathrm{Tr}[\Gamma_{L0}G_0\Gamma_{R0}(G_0)^\dagger] + \mathrm{Tr}[\Gamma_{L0}G_0\Gamma_{R0}(G_1(E))^\dagger] \\
&\quad + \mathrm{Tr}[\Gamma_{L0}G_1(E)\Gamma_{R0}(G_0)^\dagger] \\
&\quad + \mathrm{Tr}[\Gamma_{L0}G_1(E)\Gamma_{R0}(G_1(E))^\dagger] \\
&= T_{00} + T_{01}(E) + T_{10}(E) + T_{11}(E) \equiv T_{\mathrm{sum}}(E),
\end{aligned} \tag{9}$$

where T_{00} is a constant and $T_{\mathrm{sum}}(E)$ gives the approximation of transmission curve $T(E)$ about a single, isolated resonance. Substituting the expression of $G_1(E)$ into the above, we have

$$\begin{aligned}
T_{01}(E) &= T_{01}(E_0)\frac{E_0 - E_\alpha - i\gamma_\alpha}{E - E_\alpha - i\gamma_\alpha}, \\
T_{10}(E) &= T_{10}(E_0)\frac{E_0 - E_\alpha + i\gamma_\alpha}{E - E_\alpha + i\gamma_\alpha}, \\
T_{11}(E) &= T_{11}(E_0)\frac{(E_0 - E_\alpha)^2 + \gamma_\alpha^2}{(E - E_\alpha)^2 + \gamma_\alpha^2},
\end{aligned}$$

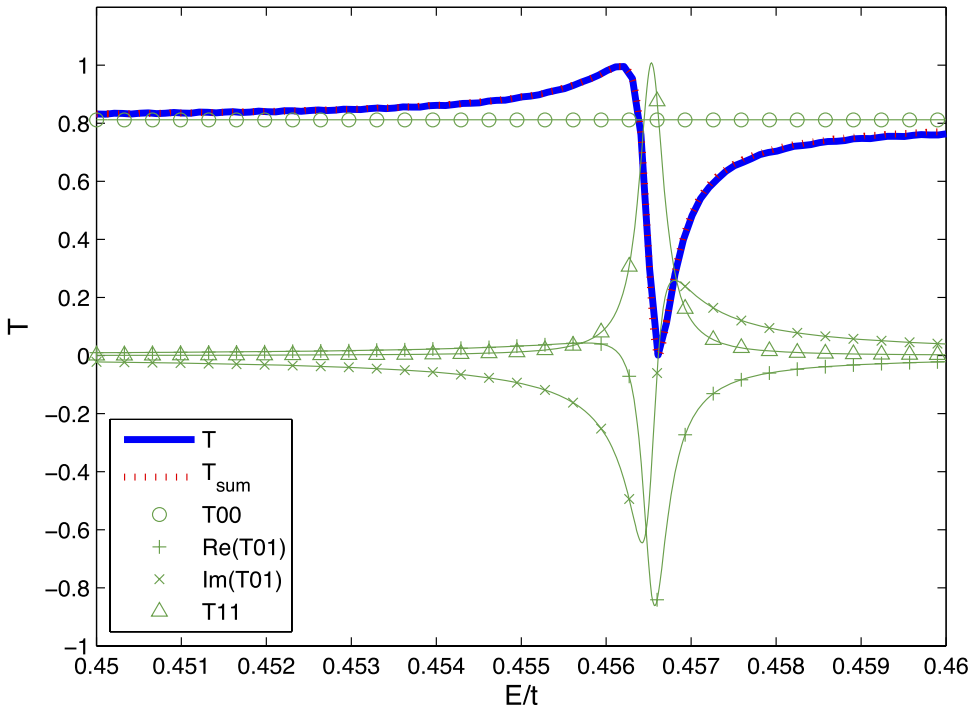

FIG. 4. A demonstration of the energy variations of the different terms in the expansion expression (9) with results from direct numerical calculation. Since $T_{10}(E) = T_{01}(E)^{\dagger}$, it is only necessary to plot $T_{01}(E)$.

where $T_{01}(E_0)$, $T_{10}(E_0)$, and $T_{11}(E_0)$ can be evaluated numerically. Figure 4 shows the energy variations of different terms in the expansion expression (9). We observe that the numerical value of $T_{11}(E)$ is comparable with those of $T_{01}(E)$ and $T_{10}(E)$, and $T_{01}(E) = T_{10}(E)^*$, where * denotes complex conjugate. Substituting these expressions into T_{sum}, we obtain

$$\begin{aligned} T_{\text{sum}}(E) = T_{00} + \frac{1}{(E-E_\alpha)^2+\gamma_\alpha^2} \times \\ \Big[\Big(T_{01}(E_0)+T_{10}(E_0)\Big)(E_0-E_\alpha)(E-E_\alpha) \\ +T_{11}(E_0)(E_0-E_\alpha)^2 \\ +i\gamma_\alpha(E-E_0)\Big(T_{10}(E_0)-T_{01}(E_0)\Big) \\ +\gamma_\alpha^2\Big(T_{01}(E_0)+T_{10}(E_0)+T_{11}(E_0)\Big)\Big]. \end{aligned}$$

Without loss of generality, we set $E_0 = E_\alpha$, leading to

$$\begin{aligned} T_{\text{sum}}(E) &= T_{00} + \frac{1}{(E-E_\alpha)^2+\gamma_\alpha^2} \times \\ &\quad \Big[i\gamma_\alpha(E-E_0)\Big(T_{10}(E_0)-T_{01}(E_0)\Big) \\ &\quad +\gamma_\alpha^2\Big(T_{01}(E_0)+T_{10}(E_0)+T_{11}(E_0)\Big)\Big], \\ &= T_{00} + \frac{T_{01}(E_0)+T_{10}(E_0)+T_{11}(E_0)}{(E-E_\alpha)^2+\gamma_\alpha^2} \\ &\quad \times\Big[i\gamma_\alpha(E-E_0)\frac{T_{10}(E_0)-T_{01}(E_0)}{T_{01}(E_0)+T_{10}(E_0)+T_{11}(E_0)} \\ &\quad +\gamma_\alpha^2\Big]. \end{aligned}$$

Letting

$$\begin{aligned}\Delta T &= T_{01}(E_0) + T_{10}(E_0) + T_{11}(E_0)\\ &= 2\mathrm{Re}(T_{01}(E_0)) + T_{11}(E_0),\\ q_r &= \frac{i}{2}\frac{T_{10}(E_0) - T_{01}(E_0)}{\Delta T} = \frac{\mathrm{Im}(T_{01}(E_0))_{48}}{\Delta T},\end{aligned}$$

we have

$$T_{\mathrm{sum}}(E) = T_{00} + \frac{\Delta T}{(E - E_\alpha)^2 + \gamma_\alpha^2}\left[2q_r\gamma_\alpha(E - E_0) + \gamma_\alpha^2\right].$$

Letting $E_0 = E_\alpha$ and $\varepsilon = (E - E_\alpha)/\gamma_\alpha$, we finally arrive at

$$T_{\mathrm{sum}}(E) = T_{00} + \Delta T\frac{1 + 2q_r\varepsilon}{\varepsilon^2 + 1}. \tag{10}$$

Validation of Eq. (10) is illustrated in Fig. 5, where the numerically obtained three isolated resonances from a graphene quantum dot are shown, together with the respective theoretical profiles. Excellent agreement is observed for energy around the resonance.

To compare with the Fano formula, we rewrite Eq. (10) as

$$T(E) = \left(T_{00} - \Delta T\right) + \Delta T\frac{(\varepsilon + q_r)^2}{\varepsilon^2 + 1} + \Delta T\frac{2 - q_r^2}{\varepsilon^2 + 1}, \tag{11}$$

where the second term is the standard Fano resonance profile[1] and the third term is a symmetric bias. Our Eq. (10) thus represents a more general formulation of the Fano-resonance profile, and it is consistent with previous results, e.g., the Fano resonance profiles of conductance from the scattering-matrix elements.[28,29] In the original formula $(\varepsilon + q_r)^2/(\varepsilon^2 + 1)$, the asymmetry parameter q_r is proportional to the ratio of the transmission amplitudes for the resonant and non-resonant channels,[1] and it is

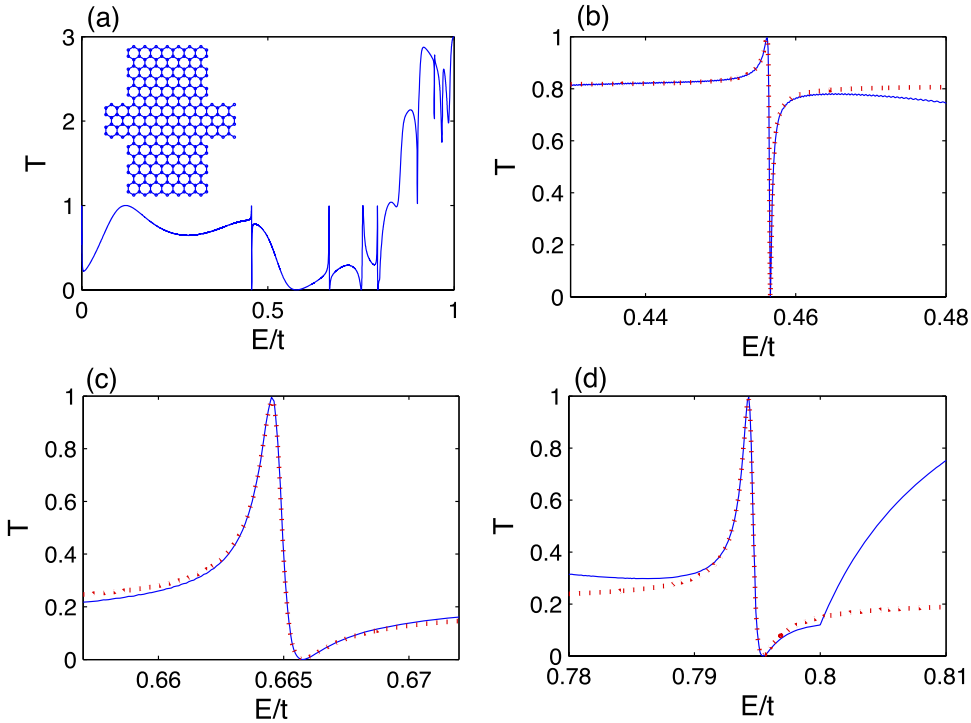

FIG. 5. Comparison of Fano resonance profiles predicted by Eq. (10) with those from direct numerical computation: (a) the graphene quantum dot system (inset) and the transmission curve for energy in the range $0 \le E/t \le 1$, where t is the nearest-neighbor hopping energy of the graphene lattice, (b-d) numerical (solid curves) and theoretical (dotted curves) profiles of three isolated resonances.

regarded as a real parameter. To see why q can take on complex values, as asserted in most existing works (e.g., those on conductance fluctuations[28]), we consider the case $q_r^2 < 2$, let $q_i = \sqrt{2 - q_r^2}$, define $q = q_r + iq_i$, and rewrite Eq. (11) as

$$T(E) = T_{00} - \Delta T + \Delta T \frac{|\varepsilon + q|^2}{\varepsilon^2 + 1}. \tag{12}$$

In previous works, q_r and q_i are related to each other in a complicated way [see, for example, Eqs. (4-12) in Ref. 28]. For $q_r < \sqrt{2}$, our formula Eq. (11) is equivalent to Eq. (12) in Ref. 28, where the first complicated term in their Eq. (12) is replaced by 2, i.e., $q_i^2 = 2 - q_r^2$. This is consistent with Fig. 4 of Ref. 28, which shows damped oscillations of q_r versus the magnetic flux with the maximum value of 1.41. This relation was also observed in previous experimental studies[15,16] of transport through a quantum dot in an Aharonov-Bohm interferometer, where it is found that $|q|$ is generally independent of the magnetic field strength and traces out a circle in the complex q plane, although $|q|$ can be larger than 2 and the center is not at the origin [Fig. 6(b-c) in Ref. 16]. The former is understandable as q is normalized by ΔT, which can be quite different depending on the specific fitting procedure employed. However, given that ΔT is fixed and determined *as in our formula*, $|q|^2$ should be 2. Thus, our derivation allows us to verify that in the normalized Fano resonance profile, the asymmetry parameter can in general be complex, regardless of the time reversal symmetry,[29] and $|q| = \sqrt{2}$. This is a universal value, independent of any details of the transport or scattering process, insofar as it can be treated by the non-equilibrium Green's function formalism. Thus we expect our formula Eq. (10) to be valid for general coherent transport through quantum dots, small scale organic crystals, single molecules, and other small-scale structures.

E. Connection to the Fano formula with complex and real asymmetric parameters

We now demonstrate a surprising consequence of Eq. (10), bridging of the Fano formulas with complex and real asymmetry parameter. In particular, we can show that the standard Fano formula with complex q parameter is equivalent to Eq. (10), and using another transformation, Eq. (10) is equivalent to the standard Fano formula with real q parameter. The indication here is that the Fano formulas with complex and real q parameters are connected through Eq. (10). Thus in an experimental fitting both real and complex q values are meaningful, and they give essentially the same physics.[49]

The Fano formula with complex asymmetric parameter has the form

$$T = |t_d|^2 \frac{|\varepsilon + q'|^2}{\varepsilon^2 + 1}, \tag{13}$$

where $|t_d|^2$ is the direct transmission without the presence of a scattering region, q' is the complex asymmetric parameter. To see its relation with Eq. (10), we can write

$$T_{00} + \Delta T \frac{1 + 2q_r\varepsilon}{\varepsilon^2 + 1} = |t_d|^2 \frac{|\varepsilon + q'|^2}{\varepsilon^2 + 1}. \tag{14}$$

Expanding both sides and letting the coefficients of different ε terms be equal, we obtain

$$\begin{aligned} T_{00} &= |t_d|^2, \\ \Delta T &= |t_d|^2(|q'|^2 - 1), \\ q_r &= q_r'/(|q'|^2 - 1), \end{aligned}$$

or

$$\begin{aligned} |t_d|^2 &= T_{00}, \\ q_r' &= \Delta T q_r / T_{00}, \\ q_i' &= \sqrt{1 + \Delta T/T_{00} - q_r^2(\Delta T/T_{00})^2}, \end{aligned}$$

where the parameters of Eq. (10) can be expressed by the parameters for Fano formula with complex asymmetric parameters, and vice versa. That is, the two are equivalent. Moreover, from the relation

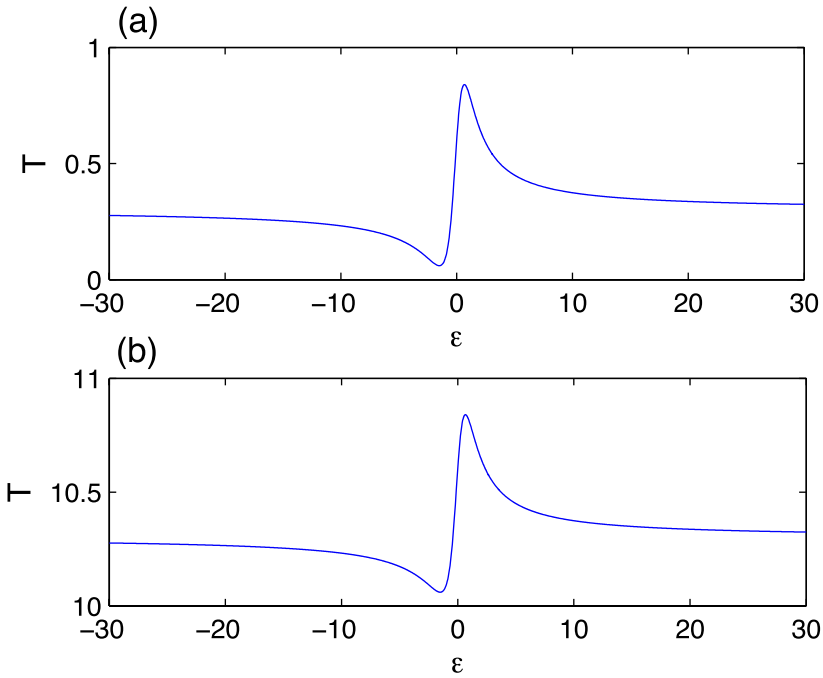

FIG. 6. For a single resonance given by Eq. (10), (a) $T_{00} = 0.3$, $\Delta T = 0.3$, $q_r = 1.2$, the resulting parameters for Eq. (13) are $|t_d|^2 = 0.3$, $q'_r = 1.2$, $q'_i = 0.748$. (b) $T_{00} = 10.3$, $\Delta T = 0.3$, $q_r = 1.2$, the resulting parameters for Eq. (13) are $|t_d|^2 = 10.3$, $q'_r = 0.035$, $q'_i = 1.014$.

we see that $|q'| = \sqrt{1 + \Delta T/T_{00}}$. When T_{00} (or $|t_d|^2$) is large, since ΔT is on the order of one, q'_r is close to zero while q'_i is close to 1. This may be misleading because for $q'_i \gg q'_r$, it may appear that the resonance is almost symmetric as discussed in previous studies,[35] but this may not be the case. Figure 6 shows the resonance profile for two cases, one with $T_{00} = 0.3$ (a) and another with $T_{00} = 10.3$ (b), with ΔT and q_r being fixed. One can see that, since only T_{00} is different, the resonance profile only has a shift for the two cases, and it has a strong asymmetric form. However, the resulting (q'_r, q'_i) for Eq. (13) are (1.2, 0.748) for (a) and (0.035, 1.014) for (b), indicating an asymmetric form for the former and a symmetric form for the latter.[35] Thus, although the two cases has the same resonant form, one may not be able to see that from the numerical values of (q'_r, q'_i) as they change drastically.

When there is only *one* transmitting mode in the leads, the maximum transmission is 1. In this case, when time reversal symmetry is present, the asymmetric parameter q' can be chosen to be real[35] ($q'_i = 0$). To distinguish with the above discussions, we use the symbol q for the real asymmetric parameter. This leads to

$$1 + \Delta T/T_{00} - q_r^2(\Delta T/T_{00})^2 = 0,$$

or

$$q_r^2 = (T_{00}/\Delta T)^2 + T_{00}/\Delta T.$$

Since $q_r = \mathrm{Im}(T_{01}(E_0))/\Delta T$, this yields

$$(\mathrm{Im}T_{01})^2 = T_{00}^2 + T_{00}\Delta T.$$

The relations between the parameters are

$$\begin{aligned} T_{00} &= |t_d|^2, \\ \Delta T &= |t_d|^2(q_r^2 - 1), \\ q_r &= q/(q^2 - 1), \end{aligned}$$

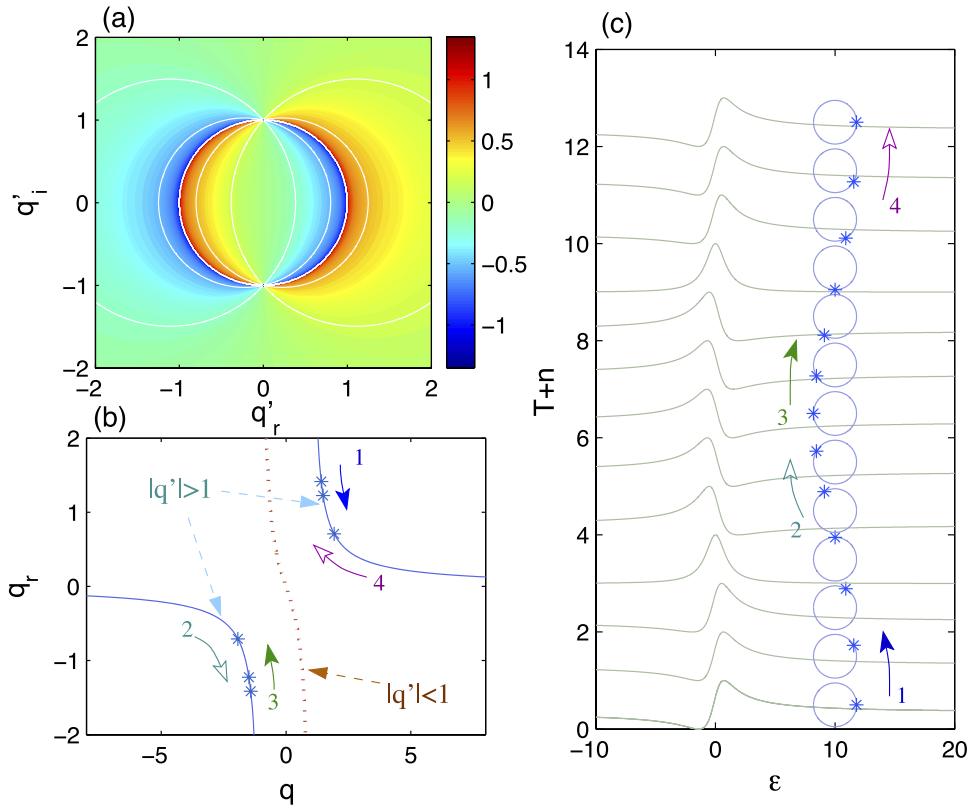

FIG. 7. (a) Contour plot of q_r on the complex asymmetry parameter q' plane. Note that q_r diverges on the unit circle $|q'| = 1$. For better visualization, for $|q_r| > 1$, it is normalized to $\text{sign}(q_r)[1+\log_{10}|q_r|]$. (b) q_r versus the real asymmetry parameter q, where it has two branches, $|q| > 1$ (solid blue curves) and $|q| < 1$ (dashed brown curve), corresponding to $|q'| > 1$ and $|q'| < 1$ in panel (a), respectively. The asterisks indicate the calculated values of q_r and q from the corresponding q', i.e., asterisks in (c). The sequence numbers (1-4) indicate the correspondence to the change complex asymmetry parameter q' in (c). (c) Transmission (shifted) versus normalized energy demonstrating Fano profiles with a complex asymmetry parameter q' (asterisk) circulating one cycle, where $|q'| = \sqrt{2}$, thus $q_r = q'_r$.

or,

$$|t_d|^2 = T_{00},$$
$$q = \Delta T q_r / T_{00},$$

To view the relation more directly, we can rewrite the above equations as follows. With $q' = q'_r + iq'_i$ and $q_r = q'_r/(|q'|^2 - 1)$ (Fig. 7(a)), we have,

$$\frac{1 + 2q_r\varepsilon}{1 + \varepsilon^2} = \left[\frac{|\varepsilon + q'|^2}{1 + \varepsilon^2} - 1\right] \cdot \frac{1}{|q'|^2 - 1}, \tag{15}$$

where the left-hand side has the form of Eq. (10), and there is no constraint on q'. With $q_r = q/(q^2 - 1)$ or $q = 1/(2q_r) \pm \sqrt{1/(4q_r^2) + 1}$ (Fig. 7(b)), we have

$$\frac{1 + 2q_r\varepsilon}{1 + \varepsilon^2} = \left[\frac{(\varepsilon + q)^2}{1 + \varepsilon^2} - 1\right] \cdot \frac{1}{q^2 - 1}. \tag{16}$$

Note that the offset on the right-hand side can be moved to the left side. The relation between q and q_r is shown in Fig. 7(b). It has two separate branches, i.e., for $|q| > 1$ and $|q| < 1$, where the latter flips the shape as the factor $q^2 - 1$ is negative. When the complex parameter $q' = q'_r + iq'_i$ is given, q_r can be uniquely determined. However, when q_r is given, q'_r and q'_i cannot be determined uniquely, but trace out a circle: $(q'_r - 1/(2q_r))^2 + q_i'^2 = 1 + 1/(4{q_r}^2)$ [see the contour lines in Fig. 7(a)]. Although

different q' on the circle may lead to distinct Fano profiles, they will collapse to a single curve determined by q_r by applying a proper shift and scaling. In Ref. 30, it is found that such a parameter q' corresponds to a dephasing process [Eq. (7) in Ref. 30]. This implies that, although dephasing breaks TRS and the resonance profile may look quite different for different values of q', it leaves clear footprints that all the profiles during a dephasing process can be tracked back to a single profile by simple rescaling and shifting. In situations where $|q'|$ is a constant, q'_r is proportional to q_r, and the change of sign in q_r indicates a sign change in q'_r as well. Thus the sign change in q'_r can simply be revealed from the incline of the resonance profile.[32] Figure 7(c) shows a series of Fano profiles with complex asymmetry parameter q' and $|q'| = \sqrt{2}$ (so $q_r = q'_r$). The calculated values of q_r and q are plotted on the $q_r(q)$ curves of Fig. 7(b). The corresponding changes in q and q_r, when q' circulates the cycle, are indicated by the sequence numbers. A similar discussion linking an expression similar to Eq. (10) to the real q-parameter Fano formula was provided by Shore in 1967.[50]

The above argument indicates that, in the experimental analysis of conductance or transmission resonance, the standard Fano formula with either real or complex q parameter can be chosen, provided that an offset can be applied. An alternative method is to fit with our formula Eq. (10). A general conclusion is that, regardless of whether TRS is present or broken, the transmission resonance profile can always be fitted by the Fano formula with real q parameter,[49] although in certain cases the employment of complex q parameter may be more convenient, especially in applications such as probing decoherence.[30]

III. WIDTH OF THE FANO RESONANCE

A. The expression of the width

In Eq. (10), the energy is normalized by γ_α, thus γ_α characterizes the width of the transmission resonance. In the following we shall develop a perturbation theory to calculate γ_α.

Regarding the conductor as a closed system, the Hamiltonian matrix H_C is Hermitian with a set of real eigenenergies and eigenfunctions:

$$H_C\psi_{0\alpha} = E_{0\alpha}\psi_{0\alpha}, \alpha = 1, \ldots, N, \tag{17}$$

where N is the number of points in the discretized conductor. The eigenstates $\{\psi_{0\alpha}|\alpha = 1, \ldots, N\}$ are orthogonal and complete, thus they form a basis in the $\Re^N$ space for the discrete spacial configuration of the wavefunctions. Recall that

$$[H_C + \Sigma]\Psi_\alpha = \varepsilon_\alpha\Psi_\alpha, \tag{18}$$

$$\varepsilon_\alpha = E_\alpha - i\gamma_\alpha, \alpha = 1, \ldots, N, \tag{19}$$

Since the self-energy matrix Σ has only nonzero elements in the subblock of boundary points connecting with the leads, for most of the eigenstates it can be treated as a perturbation. Thus for a given eigenstate α, we have

$$\varepsilon_\alpha = E_{0\alpha} - \Delta_\alpha - i\gamma_\alpha, \tag{20}$$

$$\Psi_\alpha = \psi_{0\alpha} - \delta_r\psi_{\alpha r} - i\delta_i\psi_{\alpha i}, \tag{21}$$

where Δ_α, γ_α, δ_r and δ_i are small quantities, $E_{0\alpha} - \Delta_\alpha = E_\alpha$, and $\psi_{\alpha r(i)}$ are the normalized perturbations for the real (imaginary) part of the eigenfunction $\psi_{\alpha 0}$.

Substituting Eqs. (20) and (21) back into Eq. (18) yields

$$(H_C + \Sigma)(\psi_{0\alpha} - \delta_r\psi_{\alpha r} - i\delta_i\psi_{\alpha i}) =$$
$$(E_{0\alpha} - \Delta_\alpha - i\gamma_\alpha)(\psi_{0\alpha} - \delta_r\psi_{\alpha r} - i\delta_i\psi_{\alpha i}).$$

Neglecting the second-order terms on both sides and using Eq. (17), we get

$$H_C(\delta_r\psi_{\alpha r} + i\delta_i\psi_{\alpha i}) - \Sigma\psi_{0\alpha} \approx$$
$$(\Delta_\alpha + i\gamma_\alpha)\psi_{0\alpha} + E_{0\alpha}(\delta_r\psi_{\alpha r} + i\delta_i\psi_{\alpha i}).$$

Projecting both sides of the above equation to state α, i.e., $\langle\psi_{0\alpha}|\cdot\rangle$, we obtain

$$\Delta_\alpha + i\gamma_\alpha \approx -\langle\psi_{0\alpha}|\Sigma|\psi_{0\alpha}\rangle. \tag{22}$$

This gives the first-order approximation of the shift in the eigenenergy caused by the coupling with the leads. More explicitly, we can write[51–53]

$$\gamma_\alpha \approx -\mathrm{Im}(\langle\psi_{0\alpha}|\Sigma|\psi_{0\alpha}\rangle) = -\langle\psi_{0\alpha}|\mathrm{Im}(\Sigma)|\psi_{0\alpha}\rangle. \tag{23}$$

Since $\Gamma = \Gamma_L + \Gamma_R = i(\Sigma - \Sigma^\dagger) = -2\mathrm{Im}(\Sigma)$, we have

$$\gamma_\alpha \approx \frac{1}{2}\langle\psi_{0\alpha}|\Gamma|\psi_{0\alpha}\rangle. \tag{24}$$

Since the self-energy characterizes the coupling between the conductor and the leads, γ_α can be regarded as the tunneling rate of the state Ψ_α, the eigenstate of the non-Hermitian Hamiltonian $H_C + \Sigma$. We see that γ_α is determined by the imaginary part of the self-energy Σ (or the coupling matrix Γ) and the corresponding eigenfunction $\psi_{0\alpha}$ of the isolated conductor. Since Σ (Γ) only has nonzero elements at the boundary points of the conductor connecting with the leads, only the values of $\psi_{0\alpha}$ on the same set of points, i.e., the boundary points, contribute to γ_α. Therefore localized states, typically with small $\psi_{0\alpha}$ values at the boundary points, have small γ_α thus generate sharp resonances.

Figure 8 shows, for a small graphene quantum dot, the correspondence between the transmission fluctuation and the calculated values of ε_α. The self-energy Σ is evaluated at $E_0 = 0.563t$ (somewhat arbitrary), and the values of ε_α are then calculated as the eigenvalues of the non-Hermitian Hamiltonian $H_C + \Sigma$. The positions of the resonances agree well with those from E_α. In principle, the plots are

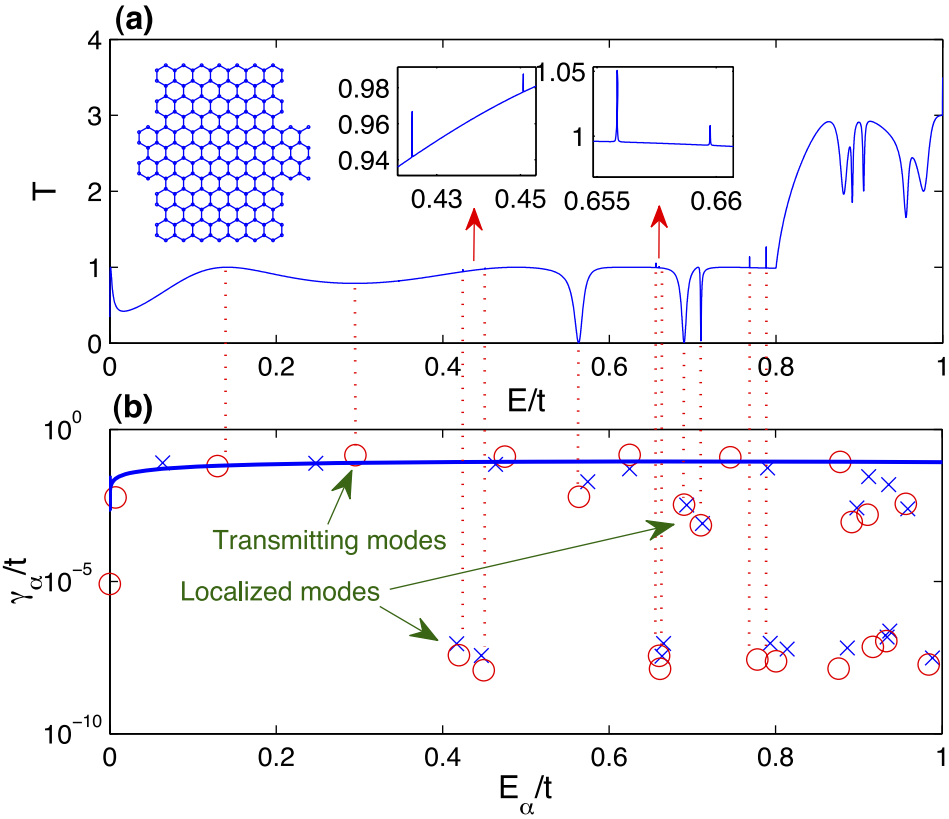

FIG. 8. For a graphene quantum dot, (a) transmission T versus energy E, (b) the real and imaginary parts of the eigenenergy ε_α. The circles denote the eigenenergy values calculated directly from the non-Hermitian Hamiltonian of the entire open system: $[H_C + \Sigma]\Psi_\alpha = \varepsilon_\alpha\Psi_\alpha$, where $E_0 = 0.563t$ is used for calculating the self-energy. The crosses represent results from our first-order perturbation theory. The blue solid curve shows the line shape obtained by a further perturbation analysis of the self-energy. The dotted vertical lines are for eye guidance.

only accurate for the eigenenergies where E_α is close to E_0 because Σ and hence ε_α are all dependent upon the energy E. But we find that, even if E_α is far from E_0, we still obtain reasonable agreement, which can be attributed to the slow variation of the self-energy Σ with the energy. The blue solid curve in Fig. 8(b) is derived from a further approximation of Σ (Eq. (32)).

B. Recovery of Eq. (12) for anti-resonance and resonant transmission

When there is only one transmitting mode, a particular focus is anti-resonance and resonant transmission. Here we shall demonstrate that in such a case, our approach can also exhibit these features.

From Eq. (12), we can obtain the extreme value of transmission, as follows. First, $dT/d\varepsilon = 0$ leads to

$$\varepsilon_e = -1 \pm \sqrt{1 + 4q_r^2}/2q_r.$$

Substituting this into Eq. (12) and letting $Q = 1 + 4q_r^2$, we obtain the extreme value of transmission as

$$T_e = T_{00} + \Delta T \frac{\pm 1}{\sqrt{Q} \mp 1} 2q_r^2.$$

Note that $q_r \to 0$ leads to symmetric peak or dip, while $q_r \to \infty$ leads to the asymmetric form. For small q_r, i.e., $q_r \ll 1$ ($\mathrm{Im}(T_{01}) \ll \Delta T$), we have $\sqrt{Q} = \sqrt{1 + 4q_r^2} \approx 1 + 2q_r^2$, leading to

$$\begin{aligned} T_e &= T_{00} + \Delta T \frac{\pm 1}{2q_r^2 + 1 \mp 1} 2q_r^2 \\ &= \begin{cases} T_{00} + \Delta T, \\ T_{00} - \Delta T(2q_r^2)/(2q_r^2 + 2) \approx T_{00}. \end{cases} \end{aligned}$$

When there is only *one* transmitting mode in the leads and the TRS is preserved, for $T_{00} = 1$ and $\Delta T = -1$, we have $T_e = 0$ and 1, corresponding to an anti-resonance; while for $T_{00} = 0$ and $\Delta T = 1$, we have $T_e = 0$ and 1, corresponding to a resonant transmission.

Next we show that the above situation, e.g., $\Delta T = 1$ or -1 can arise in certain circumstances. Recall that $\Delta T = 2\mathrm{Re}T_{01}(E_\alpha)) + T_{11}(E_\alpha)$. We shall calculate $\mathrm{Re}T_{01}$ and T_{11}. For large dots and narrow leads, the self-energy Σ can be regarded as a small perturbation of H_C. For highly localized states, we have $\Psi_\alpha \approx \Phi_\alpha \approx \psi_{0\alpha}$, yielding

$$\begin{aligned} \gamma_\alpha &\approx \frac{1}{2}\langle\psi_{0\alpha}|\Gamma|\psi_{0\alpha}\rangle \\ &\approx \frac{1}{2}\langle\Phi_\alpha|\Gamma|\Psi_\alpha\rangle \\ &= \frac{1}{2}\langle\Phi_\alpha^\dagger(\Gamma_L + \Gamma_R)\Psi_\alpha\rangle \\ &= \frac{1}{2}(\gamma_{\alpha,L} + \gamma_{\alpha,R}). \end{aligned}$$

For systems with an inversion symmetry, Ψ_α and Γ will also have the same symmetry, leading to

$$\gamma_{\alpha,L} = \gamma_{\alpha,R} \approx \gamma_\alpha.$$

For $T_{11}(E_\alpha)$, we have $T_{11} = \mathrm{Tr}[\Gamma_L G_1 \Gamma_R (G_1)^\dagger]$, where the energy is evaluated at E_α and $G_1 = \Psi_\alpha\Phi_\alpha^\dagger/(i\gamma_\alpha)$. We thus have

$$\begin{aligned} T_{11} &= \mathrm{Tr}[\Gamma_L \frac{\Psi_\alpha\Phi_\alpha^\dagger}{i\gamma_\alpha}\Gamma_R\frac{\Phi_\alpha\Psi_\alpha^\dagger}{-i\gamma_\alpha}] \\ &= \mathrm{Tr}[\Gamma_L\Psi_\alpha\Phi_\alpha^\dagger\Gamma_R\Phi_\alpha\Psi_\alpha^\dagger]/\gamma_\alpha^2 \\ &= \mathrm{Tr}[\Psi_\alpha^\dagger\Gamma_L\Psi_\alpha\Phi_\alpha^\dagger\Gamma_R\Phi_\alpha]/\gamma_\alpha^2 \\ &= (\Psi_\alpha^\dagger\Gamma_L\Psi_\alpha)(\Phi_\alpha^\dagger\Gamma_R\Phi_\alpha)/\gamma_\alpha^2 \end{aligned}$$

$$\approx \gamma_{\alpha,L} \cdot \gamma_{\alpha,R}/\gamma_\alpha^2$$
$$\approx 1.$$

This has been verified numerically. Similarly, we have

$$\begin{aligned}
\mathrm{Re}T_{01} &= \mathrm{ReTr}[\Gamma_L \sum_{\beta\neq\alpha} \frac{\Psi_\beta \Phi_\beta^\dagger}{E_\alpha - E_\beta + i\gamma_\beta} \Gamma_R \frac{\Phi_\alpha \Psi_\alpha^\dagger}{-i\gamma_\alpha}] \\
&= \mathrm{ReTr}[\Gamma_L \sum_{\beta\neq\alpha} \frac{E_\alpha - E_\beta - i\gamma_\beta}{(E_\alpha - E_\beta)^2 + \gamma_\beta^2} \Psi_\beta \Phi_\beta^\dagger \Gamma_R \frac{\Phi_\alpha \Psi_\alpha^\dagger}{-i\gamma_\alpha}] \\
&\approx -\mathrm{Tr}[\Gamma_L \sum_{\beta\neq\alpha} \frac{\gamma_\beta/\gamma_\alpha}{(E_\alpha - E_\beta)^2} \Psi_\beta \Phi_\beta^\dagger \Gamma_R \Phi_\alpha \Psi_\alpha^\dagger] \\
&= -\sum_{\beta\neq\alpha} \frac{\gamma_\beta/\gamma_\alpha}{(E_\alpha - E_\beta)^2} (\Psi_\alpha^\dagger \Gamma_L \Psi_\beta)(\Phi_\beta^\dagger \Gamma_R \Phi_\alpha),
\end{aligned}$$

where $\gamma_\beta \ll |E_\alpha - E_\beta|$ has been assumed. Defining $\gamma_{\alpha\beta} = \Psi_\alpha^\dagger \Gamma_L \Psi_\beta$ and $\gamma_{\beta\alpha} = \Phi_\beta^\dagger \Gamma_R \Phi_\alpha$, we have

$$\mathrm{Re}T_{01} = -\sum_{\beta\neq\alpha} \frac{\gamma_\beta \gamma_{\alpha\beta} \gamma_{\beta\alpha}/\gamma_\alpha}{(E_\alpha - E_\beta)^2}.$$

In the case of resonance, typically $\gamma_\beta, \gamma_{\alpha\beta}, \gamma_{\beta\alpha}, \gamma_\alpha$ are small and are of the same order of magnitude. We thus have $\gamma_\beta \sim \gamma_{\alpha\beta} \sim \gamma_{\beta\alpha} \sim \gamma_\alpha \sim \gamma$, and

$$\mathrm{Re}T_{01} = -\sum_{\beta\neq\alpha} \frac{\gamma^2}{(E_\alpha - E_\beta)^2}.$$

For a system with N discrete points, $\gamma^2/(E_\alpha - E_\beta)^2$ can be much smaller than $1/N$, thus we have $\mathrm{Re}T_{01} \sim 0$ and $\Delta T \sim T_{11} \sim 1$.

For the case of anti-resonance, γ_βs can be large, and many terms need to be included, i.e., $\gamma^2/(E_\alpha - E_\beta)^2 \sim n/N$, especially for states close to α. We then have $\mathrm{Re}T_{01} \sim -1$, and $\Delta T \sim 2\mathrm{Re}T_{01} + T_{11} \sim -1$.

C. Expansion of self-energy and a further simplified expression of the width

We can go one step further by expanding the self-energy. In general, the self-energy matrix Σ can be expressed as[43]

$$\Sigma = -t \sum_p \sum_{m\in p} \chi_{m,p} \exp(ik_m a) \chi_{m,p}^\dagger, \tag{25}$$

where $\chi_{m,p}$ characterizes the eigenfunction of mode m in lead p. Note that only the values of $\psi_{0\alpha}$ on the boundary points of the conductor, say, $\psi_{0\alpha,p}$, contribute to γ_α. Since the boundary of the conductor can be set arbitrarily without affecting the transmission, we can always choose a boundary slice of points to be the same as a slice of the lead. For a slice of n discrete points, since $\{\chi_{m,p} | m = 1, \ldots, n\}$ form a complete and orthogonal basis, we can express $\psi_{0\alpha,p}$ as

$$\psi_{0\alpha,p} = \sum_m c_m^\alpha \chi_{m,p}. \tag{26}$$

Substituting Eqs. (25) and (26) into Eq. (22), we have,

$$\begin{aligned}
&\Delta_\alpha + i\gamma_\alpha \approx -\langle \psi_{0\alpha} | \Sigma | \psi_{0\alpha} \rangle \\
&= t \sum_p \langle \psi_{0\alpha,p} | \sum_{m\in p} \chi_{m,p} \exp(ik_m a) \chi_{m,p}^\dagger | \psi_{0\alpha,p} \rangle \\
&= t \sum_p (\sum_i c_i^* \chi_{i,p}^\dagger) \times (\sum_{m\in p} \chi_{m,p} \exp(ik_m a) \chi_{m,p}^\dagger)
\end{aligned}$$

$$\times(\sum_j c_j \chi_{j,p})$$
$$= t \sum_p \sum_{m,i,j\in p} c_i^* \chi_{i,p}^\dagger \chi_{m,p} \exp(ik_m a) \chi_{m,p}^\dagger c_j \chi_{j,p}.$$

Since $\chi_{i,p}^\dagger \chi_{j,p} = \delta_{ij}$, we get[51–53]

$$\Delta_\alpha + i\gamma_\alpha \approx t \sum_p \sum_{m\in p} |c_m^\alpha|^2 \exp(ik_m a), \tag{27}$$

or

$$\gamma_\alpha \approx t \sum_p \sum_{m\in p} |c_m^\alpha|^2 \sin(k_m a). \tag{28}$$

For a two-terminal quantum dot with reflection symmetry, the eigenfunction also has this symmetry, and its value on the boundary points satisfy $\psi_{0\alpha,L} = \pm\psi_{0\alpha,R}$, corresponding to even or odd parity. The self-energy matrices and the eigenfunctions χ_i for the two leads are identical, so the contributions of the first-order approximation from the two semi-infinite leads are equal. We have

$$\Delta_\alpha + i\gamma_\alpha \approx 2t \sum_{m\in p} |c_m^\alpha|^2 \exp(ik_m a), \tag{29}$$

or

$$\gamma_\alpha \approx 2t \sum_{m\in p} |c_m^\alpha|^2 \sin(k_m a). \tag{30}$$

Since $k_m a$ is determined by the Fermi energy via the dispersion relation, the value of γ_α is mostly determined by c_m^α, which is the expanding coefficient of $\psi_{0\alpha,L}$ on the transverse eigenfunction χ_m for the leads. To be specific, we can write

$$\psi_{0\alpha} = \begin{pmatrix} \psi_{0\alpha,L} \\ \psi_{0\alpha,dot} \\ \psi_{0\alpha,R} \end{pmatrix}. \tag{31}$$

The wave function $\psi_{0\alpha}$ is normalized, i.e., $\psi_{0\alpha}^\dagger \psi_{0\alpha} = \psi_{0\alpha,L}^\dagger \psi_{0\alpha,L} + \psi_{0\alpha,dot}^\dagger \psi_{0\alpha,dot} + \psi_{0\alpha,R}^\dagger \psi_{0\alpha,R} = 1$. For dispersive or transmitting states where $\psi_{0\alpha}$ takes on similar values on all points, the values on the boundary points are of the order of $1/\sqrt{N}$. However, a localized state will have a large value of $\psi_{0\alpha,dot}$ on a small subset of points, e.g., points on a particular classically stable orbit in the dot. This will then lead to small values of $\psi_{0\alpha,L}$ on the boundary points, resulting in small c_m^α and γ_α. This localization effect can be so strong that the values of γ_α are several orders-of-magnitude smaller, i.e., $10^{-5}t$ versus $10^{-2}t$ for the dispersive states (See Refs. 51–53 and also Fig. 3 in the main text).

When the leads are narrow, they will have only one transverse mode in a relatively large energy interval. In this case, the summation (30) has only one term and becomes

$$\gamma_\alpha \approx 2t|c_m^\alpha|^2 \sin(k_m a) \sim \sin(ka), \tag{32}$$

where $k(E)$ can be obtained from the dispersion relation, and we have assumed that the dependence of c_m^α on α is weak and so can be treated as a constant. Figure 3 in the main text shows the results of Eq. (32) together with the numerical results. We find a good agreement.

IV. CONCLUDING REMARKS

To summarize, we have developed a framework based on coherent quantum transport to establish the universality of the Fano resonance profile. Technically, our approach is to decompose the non-equilibrium Green's function into a fast and a slow components, enabling us to derive a general formula for the resonance. In cases where the fast component of the Green's function is dominated by

only one eigenstate of the conductor, the Fano resonance profile can be described by Eq. (10), which is equivalent to the Fano formula with either real or complex q parameter. We have provided simple mathematical transformations to connect the three forms. Thus, for a given resonance, depending on the choice of the free parameters, it can be fitted by any of the three formulas with distinctly different q values. Note that for certain cases where the consideration of time-reversal symmetry is important, the choice of Fano formula with complex q parameter is preferred.[15,16,30] However, as we have demonstrated in this work, if a resonance can be fitted by Fano formula with complex q parameter, then it can also be fitted by Eq. (10) and consequently the Fano formula with a real q parameter. Therefore, a fitting to Fano formula with *complex* q parameter is not absolutely necessary for any single resonance, although a series of resonances may preferably be fitted by the formulas with a a set of complex q parameters, which may be particularly useful in probing phenomena such as decoherence.[30]

The width of the resonance, which also characterizes the lifetime of the eigenstate in the originally closed conductor, is mainly determined by the eigenfunction of the conductor, especially the values at the boundary, given that the self-energies vary slowly with the energy. For dispersive or transmitting states, the boundary values of the eigenfunction can be large, leading to a strong coupling between the conductor and the leads. Tunneling to the lead is then facilitated, resulting in a short lifetime and, consequently, in a large resonance width. The conductance curve will appear "smooth" with energy variation. In the opposite case, if a state is highly localized, i.e., on a classically stable orbit, then the eigenfunction assumes large values on this orbit, but can be extremely small anywhere else, including the boundary. The coupling of this state to the leads can be significantly weaker, leading to a long lifetime and a much smaller resonance width. In this case, the conductance curve will exhibit abrupt variations as represented by a sharp Fano resonance. This connection between the scar/pointer state and the abrupt variation in the conductance curve has been noticed before.[38–42]

While we have treated only two terminal transport systems, Fano resonance in multi-terminal systems can be treated similarly, where Eq. (10) and the interpretation of the resonant width remain valid. Due to the ubiquity of Fano resonance and the only assumption in our derivation is that the transport can be described by the Green's function formalism (which can be expanded to include decoherence in a proper way[27,30]), our formula and finding apply not only to quantum transport, but also to wave scattering phenomena arising from diverse fields such as electromagnetic waves, acoustics, and seismology.

ACKNOWLEDGEMENTS

We thank Dr. R. Yang for discussions. This work was partially supported by the NSF of China under Grants Nos. 11375074, 11422541, 11174115 and 11325417, by Doctoral Fund of Ministry of Education of China under Grant No. 20130211110008. LH and YCL were also supported by AFOSR under Grant No. FA9550-12-1-0095 and by ONR under Grant No. N00014-08-1-0627.

[1] U. Fano, Phys. Rev. **124**, 1866 (1961).
[2] A. E. Miroshnichenko, S. Flach, and Y. S. Kivshar, Rev. Mod. Phys. **82**, 2257 (2010).
[3] R. K. Adair, C. K. Bockelman, and R. E. Peterson, Phys. Rev. **76**, 308 (1949).
[4] U. Fano and J. W. Cooper, Phys. Rev. **137**, 1364 (1965).
[5] F. Cerdeira, T. A. Fjeldly, and M. Cardona, Phys. Rev. B **8**, 4734 (1973).
[6] R. Gupta, Q. Xiong, C. K. Adu, U. J. Kim, and P. C. Eklund, Nano Letters **3**, 627–631 (2003).
[7] J. Feist, F. Capasso, C. Sirtori, K. W. West, and L. N. Pfeiffer, Nature (London) **390**, 589 (1997).
[8] H. Schmidt, K. L. Campman, A. C. Gossard, and A. Imamoglu, Appl. Phys. Lett. **70**, 3455 (1997).
[9] V. Madhavan, W. Chen, T. Jamneala, M. Crommie, and S. Wingreen, Science **280**, 567 (1998).
[10] O. Újsághy, J. Kroha, L. Szunyogh, and A. Zawadowski, Phys. Rev. Lett. **85**, 2557 (2000).
[11] H. G. Luo, T. Xiang, X. Q. Wang, Z. B. Su, and L. Yu, Phys. Rev. Lett. **92**, 256602 (2004).
[12] J. Göres, D. Goldhaber-Gordon, S. Heemeyer, M. A. Kastner, H. Shtrikman, D. Mahalu, and U. Meirav, Phys. Rev. B **62**, 2188 (2000).
[13] C.-M. Ryu and S. Y. Cho, Phys. Rev. B **58**, 3572 (1998).
[14] W. Hofstetter, J. König, and H. Schoeller, Phys. Rev. Lett. **87**, 156803 (2001).
[15] K. Kobayashi, H. Aikawa, S. Katsumoto, and Y. Iye, Phys. Rev. Lett. **88**, 256806 (2002).
[16] K. Kobayashi, H. Aikawa, S. Katsumoto, and Y. Iye, Phys. Rev. B **68**, 235304(8) (2003).
[17] J. Kim, J.-R. Kim, J.-O Lee, J. W. Park, H. M. So, N. Kim, K. Kang, K.-H. Yoo, and J.-J. Kim, Phys. Rev. Lett. **90**, 166403 (2003).
[18] W. Yi, L. Lu, H. Hu, Z. W. Pan, and S. S. Xie, Phys. Rev. Lett. **91**, 076801 (2003).

[19] S. Rotter, F. Libisch, J. Burgdörfer, U. Kuhl, and H.-J. Stöckmann, Phys. Rev. E **69**, 046208 (2004).
[20] B. Luk'yanchuk, N. I. Zheludev, S. A. Maier, N. J. Halas, P. Nordlander, H. Giessen, and C. T. Chong, Nat. Mater. **9**, 707 (2010).
[21] S. Fan, W. Suh, and J. D. Joannopoulos, J. Opt. Soc. Am. A **20**, 569 (2003).
[22] L. Zhou and A. W. Poon, Opt. Lett. **32**, 781 (2007).
[23] W.-J. Chen, J. C. W. Lee, J.-W. Dong, C.-W. Qiu, and H.-Z. Wang, Appl. Phys. Lett. **98**, 081116 (2011).
[24] M. Tomita and H. Ebihara, Opt. Commun. **284**, 5513 (2011).
[25] C.-Y. Chao and L. J. Guo, Appl. Phys. Lett. **83**, 1527 (2003).
[26] S. Katsumoto, J. Phys.: Condens. Matter **19**, 233201 (2007).
[27] A. A. Clerk, X. Waintal, and P. W. Brouwer, Phys. Rev. Lett. **86**, 4636 (2001).
[28] T. Nakanishi, K. Terakura, and T. Ando, Phys. Rev. B **69**, 115307 (2004).
[29] M. Mendoza, P. A. Schulz, R. O. Vallejos, and C. H. Lewenkopf, Phys. Rev. B **77**, 155307 (2008).
[30] A. Bärnthaler, S. Rotter, F. Libisch, J. Burgdörfer, S. Gehler, U. Kuhl, and H.-J. Stöckmann, Phys. Rev. Lett. **105**, 056801 (2010).
[31] N. L. S. Martin, B. A. deHarak, and K. Bartschat, J. Phys. B: At. Mol. Opt. Phys. **42**, 225201 (2009).
[32] O. V. Misochko, M. Hase, K. Ishioka, and M. Kitajima, JETP Lett. **82**, 426 (2005).
[33] W. Porod, Z.-A. Shao, and C. S. Lent, Appl. Phys. Lett. **61**, 1350 (1992); Phys. Rev. B **48**, 8495 (1993).
[34] E. Tekman and P. F. Bagwell, Phys. Rev. B **48**, 2553 (1993).
[35] J. U. Nöckel and A. D. Stone, Phys. Rev. B **50**, 17415 (1994).
[36] B. Weingartner, S. Rotter, and J. Burgdörfer, Phys. Rev. B **72**, 115342 (2005).
[37] H. Lee, C. Jung, and L. E. Reichl, Phys. Rev. B **73**, 195315 (2006).
[38] J. P. Bird, R. Akis, D. K. Ferry, A. P. S. de Moura, Y.-C. Lai, and K. M. Indlekofer, Rep. Progr. Phys. **66**, 583–632 (2003).
[39] H. Z. Wojciech, Rev. Mod. Phys. **75**, 715 (2003).
[40] L. Huang, Y.-C. Lai, D. K. Ferry, S. M. Goodnick, and R. Akis, Phys. Rev. Lett. **103**, 054101 (2009).
[41] L. Huang, Y.-C. Lai, D. K. Ferry, R. Akis, and S. M. Goodnick, J. of Physics: Condensed Matter **21**, 344203 (2009).
[42] D. K. Ferry, L. Huang, R. Yang, Y.-C. Lai, and R. Akis, J. Phys.: Conf. Ser. **220**, 012015 (2010).
[43] S. Datta, *Electronic Transport in Mesoscopic Systems* (Cambridge University Press, Cambridge, UK, 1995).
[44] M. P. Lopez Sancho, J. M. Lopez Sancho, and J. Rubio, J. Phys. F: Met. Phys. **14**, 1205 (1984).
[45] M. P. Lopez Sancho, J. M. Lopez Sancho, and J. Rubio, J. Phys. F: Met. Phys. **15**, 851 (1985).
[46] M. B. Nardelli, Phys. Rev. B **60**, 7828 (1999).
[47] R. Landauer, Phil. Mag. **21**, 863 (1970).
[48] In general, T_{00}, ΔT and q_r are independent of each other. However, when there is only *one* transmitting mode and the system preserves TRS, the parameters are related to each other through $q_r^2 = (T_{00}/\Delta T)^2 + T_{00}/\Delta T$. In this case, a perfect transmission zero will occur at $\varepsilon_e = -q_r \Delta T/T_{00} = -\mathrm{Im}T_{01}/T_{00}$.
[49] Note that the conclusion here is valid for a general situation, especially in experiments where conductance-resonance data are usually fit using the Fano formula *with an offset*.[12,15,16,36] In the case where there is only *one* transmitting mode and Fano formula is with respect to $|t(\varepsilon)|^2 = |t_d|^2 \times |\varepsilon + q|^2/(\varepsilon^2 + 1)$ without offsets, the discussions of TRS and the complex q parameters are strictly applicable. That is, if the system preserves TRS, q will be real, leading to transmission zero for any isolated resonance. If TRS is broken, q will in general be complex, and the minimum of the transmission will not reach zero. A special case is where the system has an inversion symmetry. In this case, even if the TRS is broken, the system will be invariant under the joint operation of time reversal and spatial inversion,[35] leading to real q values and consequently zero transmission.
[50] B. W. Shore, Rev. Mod. Phys. **39**, 439 (1967).
[51] R. Yang, L. Huang, Y.-C. Lai, and C. Grebogi, EuroPhys. Lett. **94**, 40004 (2011).
[52] R. Yang, L. Huang, Y.-C. Lai, and L. M. Pecora, Appl. Phys. Lett. **100**, 093105 (2012).
[53] R. Yang, L. Huang, Y.-C. Lai, C. Grebogi, and L. M. Pecora, Chaos **23**, 013125 (2013).